



## The Effect of the Crack Initiation and Propagation on the P-Wave Velocity of Limestone and Plaster Subjected to Compressive Loading

T. Asheghi Mehmadari<sup>\*1</sup>, A. Fahimifar<sup>2</sup>, F. Asemi<sup>3</sup>

<sup>1</sup> Ph.D Student, Department of Civil & Environmental Engineering, Amirkabir University of Technology, Tehran, Iran.

<sup>2</sup> Professor, Department of Civil & Environmental Engineering, Amirkabir University of Technology, Tehran, Iran.

<sup>3</sup> Master Graduate, Department of Civil and Environmental Engineering, University of Zanjan, Zanjan, Tehran, Iran.

**ABSTRACT:** Since many large-scale projects such as tunnels, boreholes constructed for extracting gas and oil and underground excavations for the disposal of chemical wastes are being produced in high stress rock masses; it is necessary to consider the crack initiation and propagation process in rock. Various methods have been developed for monitoring the material damage and fracture. Among these methods, in recent years, the use of the variation trend of the velocity of ultrasonic waves due to the unique characteristics has attracted the attention of researchers in the field of damage mechanics. In this research, the effectiveness of this method was evaluated in the monitoring of the crack initiation and propagation process in the rock. For this purpose, the effect of crack initiation and propagation on pressure wave velocity was investigated for loading at four stress levels of 30, 50, 70 and 90% of peak strength in limestone (travertine) and six stress levels of 30, 50, 60, 70, 90 and 100% of peak strength in plaster. A microscopic thin-section of limestone sample was prepared and studied in order to clarify the cracking process after compressive loading parallel with the loading direction. The results of the research indicate that, the pressure wave velocity has increased up to a certain stress level as a result of compressive loading and then, with a higher loading, the pressure wave velocity suddenly and severely decreases. Accordingly, in the limestone to the stress level of 50% of the peak strength, the pressure wave velocity increased by about 5% and then decreases by about 50 percent with increasing load. Similarly, in plaster artificial stone up to the loading level of 70%, the wave velocity increased by about 1.6% and then suddenly decreased. In addition, the study of microscopic thin sections showed that when the limestone is subjected to stress, the cracks initiate and propagate approximately parallel with the applied load (0-10). It was also observed that under stress around the pores in the texture of the rock, concentration of stress has occurred and, cracks around these pores have grown and penetrated into the grains by breaking the bond between the grains.

### Review History:

Received: 2019-02-01

Revised: 2019-03-12

Accepted: 2019-03-13

Available Online: 2019-03-13

### Keywords:

Crack initiation and propagation

Uniaxial compressive strength

Pressure wave velocity

Limestone and plaster

## 1. INTRODUCTION

Generally, brittle rocks are broken by the initiation, propagation, and coalescence of micro-cracks caused by stress. Brace et al. (1966), Bieniawski (1967), and Martin and Chandler (1994) have divided the process of failure in brittle rocks subjected to uniaxial compressive loading into five sections [1-3]. These steps include: (1) crack closure, (2) linear elastic deformation, (3) crack initiation and stable propagation of crack, (4) crack damage and unstable propagation, and (5) failure and post-peak behavior. Accordingly, three important stress levels can be identified in the study of rock failure behavior due to compressive loading including crack initiation stress, crack damage stress and peak stress. According to the results of the researchers, the ratio of the crack initiation stress and the crack damage stress to the peak stress is about 0.3-0.6 and 0.95-0.9. In the past decades, research in this area has focused more on the

\*Corresponding author's email: T\_asheghi@aut.ac.ir

mechanism of crack propagation and the study of stress-strain behavior in rocks. However, how, time and place of crack initiation and its propagation in rocks due to pressure is still one of the unsettled questions in the field of rock damage mechanics. In order to better understand the material fracture process, researchers used various methods such as: (1) studying transparent materials such as ice and glass as brittle materials [3-7], (2) recording rock properties changes such as axial and lateral strain, sound propagation, ultrasonic wave propagation velocity during compression testing and evaluation of their relationship with the crack damage process in the rock [1, 2, 8, 9], and (3) the use of special techniques that help to observe the internal texture and micro-structure of the rock (such as computer tomography (CT-Scan)) [10-18]. The velocity of elastic waves in brittle rocks is influenced by several factors such as density, porosity, mineralogical composition, heterogeneity, weathering and lateral and axial confining pressures [19]. Despite the importance of studying



the effect of rock fracture on wave velocity in laboratory-scale brittle rocks, there is currently no adequate study in this field. Zhao et al. (2006) evaluated the ultrasonic wave attenuation along parallel fracture in an experimental study and provided a better understanding of the propagation of waves along the discontinuities [20]. Nasser et al. (2007) examined the effect of the degree of fracture (due to heat) on the pressure wave velocity by testing on the Westerly granite. In this study, they observed that thermal fractures, in addition to significantly reducing the mechanical strength of the rock, also affect its dynamic elastic properties [21]. Azhari and Hassani (2013) experimentally studied the effect of number, length and direction of artificial discontinuities on the wave velocity, and concluded that the decrease of the pressure wave velocity depends on the crack density and roughness of fractures surface [22]. Martínez-Martínez et al. (2016) evaluated the characteristics of the crack damage process during a uniaxial compressive test of low porosity carbonate rocks using ultrasonic waves and X-ray computer tomography. According to their studies, they reported that the pressure wave velocity increases during compressive loading up to the stress level where with the unstable crack growth initiates ( $\sigma_{CD}$ ). This increase in the pressure wave velocity for marble was between 15% and 30%, and for micrite limestone was between 5% and 10% of the initial value of  $V_p$ . According to Martínez-Martínez et al. (2016), when the mechanical cracks propagate unstably, the velocity stops to increase and decreases only when rock damage is very high.

Research literature studies show that despite relatively large studies on the crack initiation and propagation, their coalescence process and the formation of the fracture surface in the final stage, there are also many uncertainties in this area, especially in non-homogeneous rocks. It seems that the use of pressure wave velocity as a dynamic parameter can be efficient in better understanding the cracking process. According to what has been said, there is little experimental research available on the effect of the rock fracture mechanism on the wave velocity. In this research, in order to better understand the process of crack propagation and growth in rock, the influence of closure, initiation and propagation of crack on the pressure wave velocity has been evaluated by loading at four levels of stress of 30, 50, 70 and 90% of peak strength in limestone and six stress levels of 30, 50, 60, 70, 90 and 100% of peak strength in the plaster artificial stone.

## 2. MATERIALS AND METHODS

The present research has been carried out on artificial stones (plaster) and limestone (travertine). The limestone of Atash-kooch mine on 20 kilometers east of Mahallat city and about 5 kilometers east of Nimvar was used for this purpose. Fig. 1 shows the access road to the travertine mine of Atash-kooch and a sample of the rock cores prepared. For this purpose, suitable blocks of these rocks were selected and then cores were prepared in accordance with ISRM standard. The cores prepared to conduct rock mechanics tests have a length-to-diameter ratio of at least 2 mm and the diameter of approximately 64 mm. The end surfaces of these cores

were prepared in accordance with the International Standard for Rock Mechanics. The porosity in the studied rocks was determined to be 4-6% [23]. It should be noted that porosity in rock samples was determined using saturation method and dimensional measurement in accordance with the proposed ISRM standard. According to this method, at first, the dimensions of the sample were measured by a caliper with a precision of 0.1 mm and the total volume of the sample ( $V$ ) was obtained. The sample was then saturated in water and in a vacuum of less than 800 Pascal for one hour. During this period, the specimen must be moved alternately so that the air bubbles are removed. The surface of the sample was dried by wet cloth after leaving the water and then the saturated sample mass with the dried surface ( $M_{sat}$ ) was measured. Finally, the sample was transferred to the oven at 105 °C and kept inside the oven until reaching a constant weight. Then, it was cooled for 30 minutes in a desiccator and the solid mass or dry mass of the sample ( $M_s$ ) was measured. The following relationships were used to determine porosity:

$$V_V = \frac{M_{sat} - M_s}{\rho_w} \quad (1)$$

$$n = \frac{100V_V}{V} \quad (2)$$

For the preparation of plaster artificial stone samples, the plaster to water ratio of 3 to 1 was used (Fig. 1b and c). The length to diameter ratio in plaster samples was 2 and their diameter was 70 mm.

Uniaxial compressive strength tests were performed for all specimens based on the proposed ISRM methods [24]. These experiments were carried out using the DARTEC-9600 servo-control machine available in the Amirkabir University of Technology Rock Mechanics Laboratory with loading capacity of 1000 KN. Loading of specimens was performed in displacement control mode at constant rate of 0.002 mm/s. Axial strain and axial stress data were recorded during the experiments. In this study, the pressure wave velocity was measured using the Tico device. It should be noted that the ISRM, 2014 standard was used to measure wave velocity. As mentioned earlier, in this study, limestone subjected to various compressive loadings of 30, 50, 70 and 90% of the peak load and plaster stone subjected to various compressive loadings of 30, 50, 60, 70, 90 and 100% of the peak load were used to study the process of rock damage initiation and propagation. And loading would stop at these load levels and, the pressure wave velocity was measured on these specimens using the ultrasonic device. For this purpose, new samples were used at each stress level. It should be noted that for limestone, loading was done up to 90% of the peak strength of the specimen and a little before its final fracture so that the specimen could be removed from the loading jaw in order to determine the pressure wave velocity. For this purpose, the test for loading 90% of peak stress in limestone was repeated three times. In the case of plaster, due to their plasticity characteristics, they

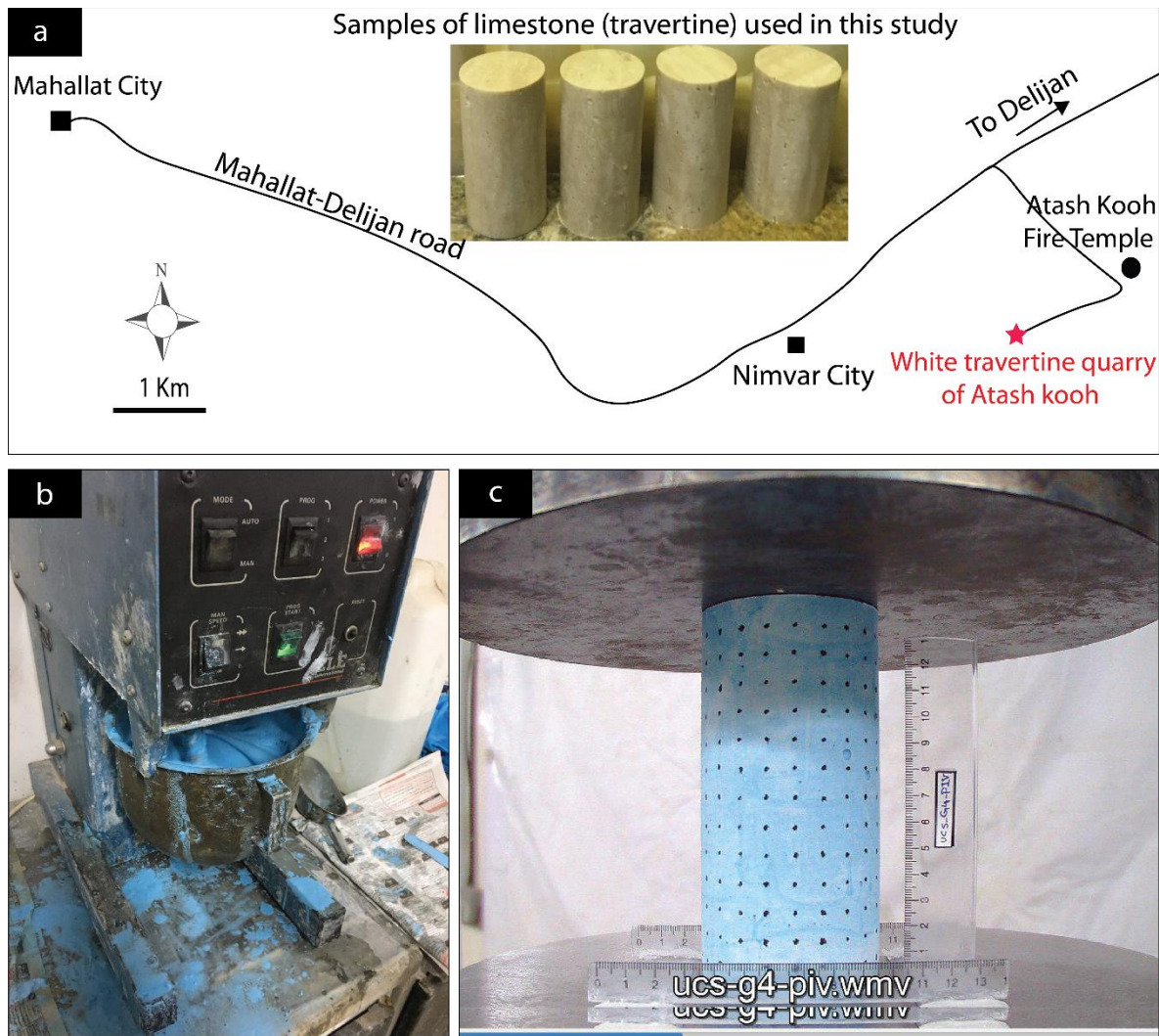


Fig. 1: (a) The access road to the travertine mine and a sample of rock for the present study; (b) the supply of plaster artificial stone at plaster to water ratio of 3 to 1; and (c) plaster subjected to compressive loading.

Table 1: Average values of the peak strength determined for limestone and plaster used in this study

Rock type	Sample	Uniaxial Compressive Strength (UCS)	Mean uniaxial compressive strength (standard deviation in parenthesis)
Limestone	UCS-T1	62	59.2 ( $\pm 1.70$ )
	UCS-T2	59	
	UCS-T3	57.5	
	UCS-T4	58.3	
plaster	UCS-G1	16.5	16.38 ( $\pm 0.34$ )
	UCS-G2	16.5	
	UCS-G3	15.8	
	UCS-G4	16.7	

did not failure after reaching their maximum strength, and there was a possibility to determine the pressure wave velocity.

In this study, four uniaxial compressive tests were first performed to determine the peak strength of the studied

rocks and the mean peak stress results were used to determine loading stopping stages. In Table 1, the peak strength values for the samples used to determine the mean peak strength have been presented.

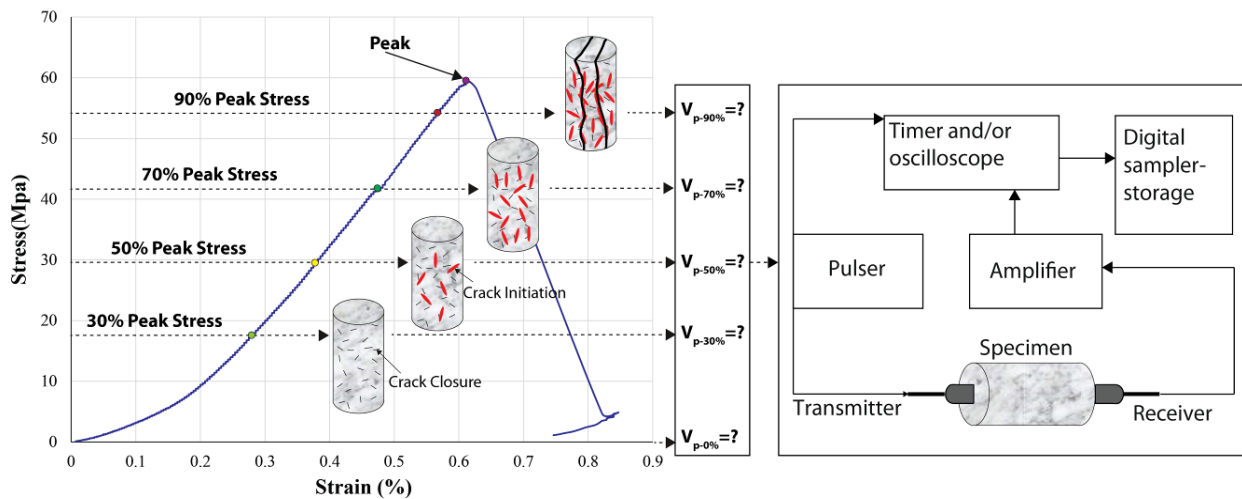


Fig. 2: Experimental program of the present study

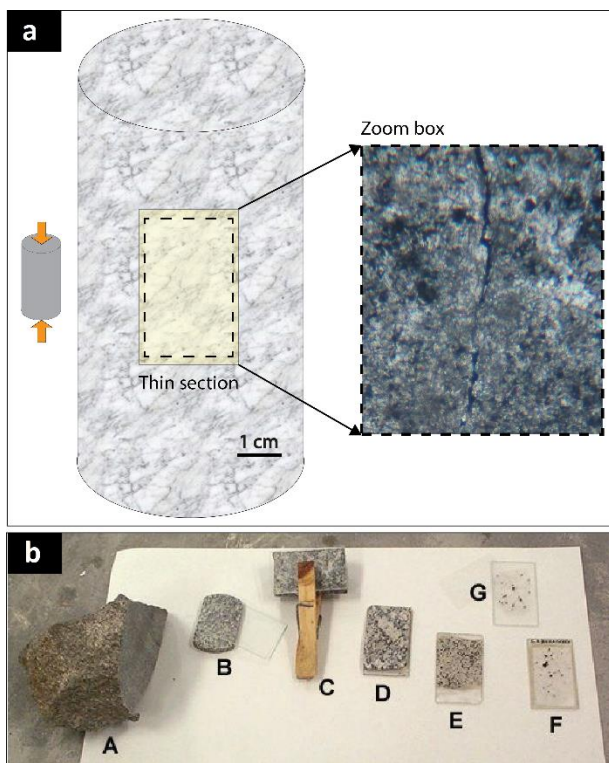


Fig. 3: (a) Schematic view of the thin section of the specimen after the uniaxial compression test along with loading and (b) order of the steps of preparing thin sections from rock to thin section

Fig. 2 shows schematically the experimental program of the present study.

In this study, thin sections were prepared after uniaxial compression test from microscopic fracture areas in order to study the microstructure of limestone and to investigate the cracking process caused by compressive loading. Fig. 3a shows the schematic image of the thin section of the sample after the uniaxial compression test along with the loading direction. It should be noted that in order to prepare a thin section, first the rock sample is cut into a rectangular cube (Fig. 3b). After

cutting, the surface of the block is completely rubbed using silicon carbide powders. The surface is then rubbed with a twin glue to the slide and placed for a few hours away from light and heat to make the adhesive very hard. Thereafter, the thickness of the added block installed on the slab is cut and is rubbed to reduce the thickness to a standard limit (about 30 microns) with abrasive powders. After the abrasion stage, it is pasted to the surface of the slide sample and the specimen is fixed.

### 3. EVALUATION OF RESULTS

The results obtained in this study have been presented in Tables 2, 3 and Fig. 4 for limestone and plaster artificial stone. Generally, the variations in the pressure wave velocity along with the loading are similar to those of the two samples (limestone and plaster artificial stone). As shown in Fig. 4a, the  $V_p$  graph for the two types of rock can be divided into two important stages: (1) At this stage, the pressure wave velocity increases by increasing the loading to a certain stress level and then (2) with a higher loading, the pressure wave velocity will fall suddenly and severely. This observation indicates the impressionability of the pressure wave velocity by the increase in the density of micro-crack in the rock. In other words, with the initiation, propagation and coalescence of the cracks caused by the loading, pressure wave velocity in parallel with the loading initially increases and then decreases. In accordance with Table 2 and Fig. 4, the value of  $V_p$  for limestone in the first step up to the stress level of 50% of the peak strength increased (by about 5%) and further decreased by about 50%. Similar to what has been mentioned for limestone, in plaster artificial stone, the P-wave velocity has increased by about 1.6% up to the loading of 70% and then suddenly decreases. This finding is similar to the results of Martínez-Martínez et al. (2016) [13]. Investigating the relationship between stress-strain curve in limestone and plaster stone and the variation trend of the pressure wave velocity indicate that with the initiation and stable propagation of the micro-crack in the rock, the P-wave velocity is increased afterwards, the pressure wave velocity suddenly and significantly decreases with

**Table 2: Results of the test of pressure wave velocity at four loading levels in uniaxial compression test for limestone**

Sample	$\sigma(MPa)$	P-wave velocity (m/s)				Average P-wave velocity (m/s)
UT-T1-0%	0	4700	4700	4700	4700	4700
UT-T1-30%	17.83	4810	4840	4840	4840	4832.5
UT-T1-50%	29.71	4920	4920	4920	4920	4920
UT-T1-70%	41.59	4770	4810	4770	4770	4780
UT-T1-90%	53.48	3190	3110	3110	3120	3132.5

**Table 3: Results of the test of pressure wave velocity at six loading levels in uniaxial compression test for plaster**

Sample	$\sigma(MPa)$	P-wave velocity (m/s)				Average P-wave velocity (m/s)
UT-G1-0%	0	1800	1800	1800	1800	1800
UT-G1-30%	4.96	1800	1800	1800	1800	1800
UT-G1-50%	8.27	1810	1810	1810	1810	1810
UT-G1-60%	9.92	1820	1820	1820	1820	1820
UT-G1-70%	11.58	1830	1830	1830	1830	1830
UT-G1-90%	14.89	1770	1780	1780	1780	1777.5
UT-G1-100%	16.54	1660	1660	1670	1670	1665

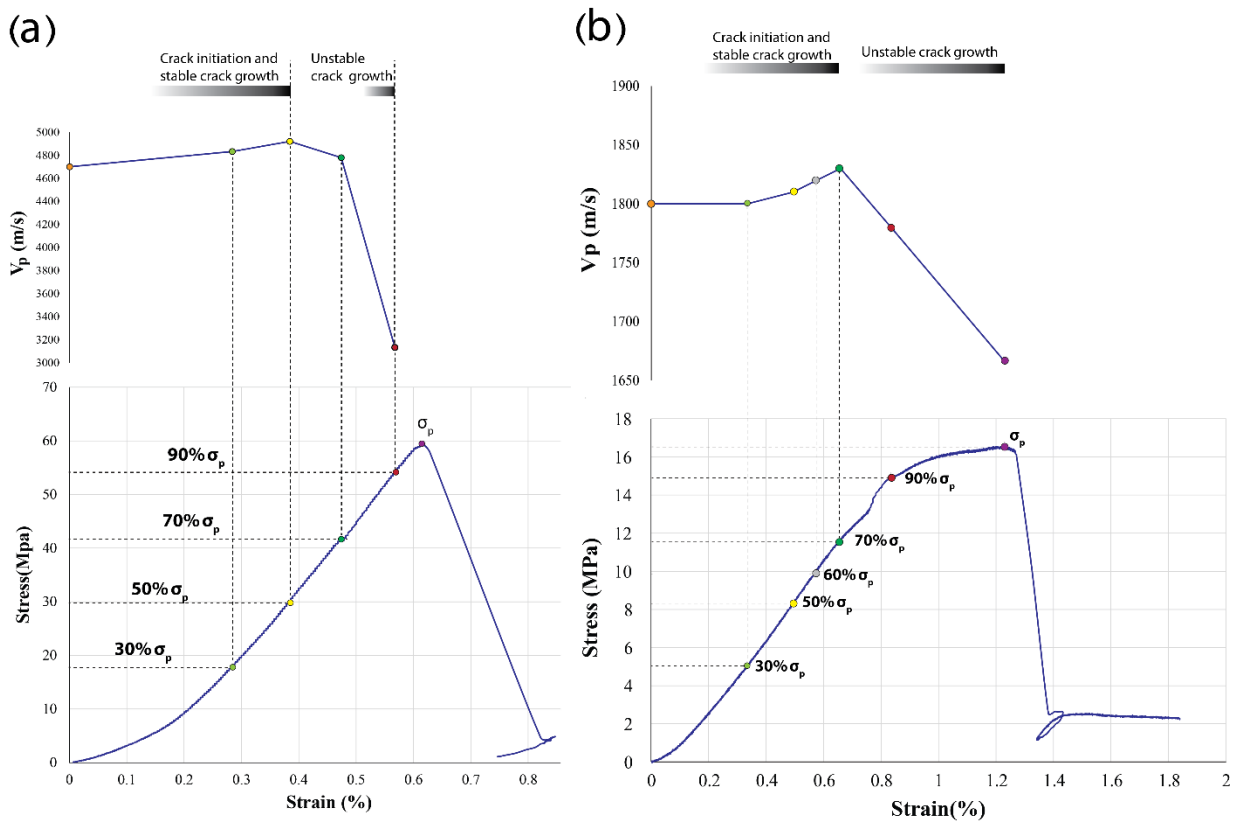


**Fig. 4: Pressure wave velocity variations due to the loading of (a) limestone up to 30, 50, 70 and 90% of the peak stress; and (b) plaster artificial stone to 30, 50, 60, 70 and 90 and 100% of the peak stress.**

increasing density of micro-cracks and the rapid propagation and ultimately coalescence of the micro-cracks created by the compressive loading. The initial increase in the pressure wave velocity reflects the elastic compaction of the intact rock, and then the initiation and propagation of the micro-cracks slowly in parallel with the loading direction. Then, a sudden decrease in the pressure wave velocity indicates a sudden

increase in crack density in the rock. According to the results, it can be said that the determination of the pressure wave velocity can be helpful in a better understanding of the crack initiation and their propagation stages under compressive loading. Of course, this requires more research. It seems that the use of cube samples to study the effect of the initiation and propagation of cracks on the wave velocity in perpendicular

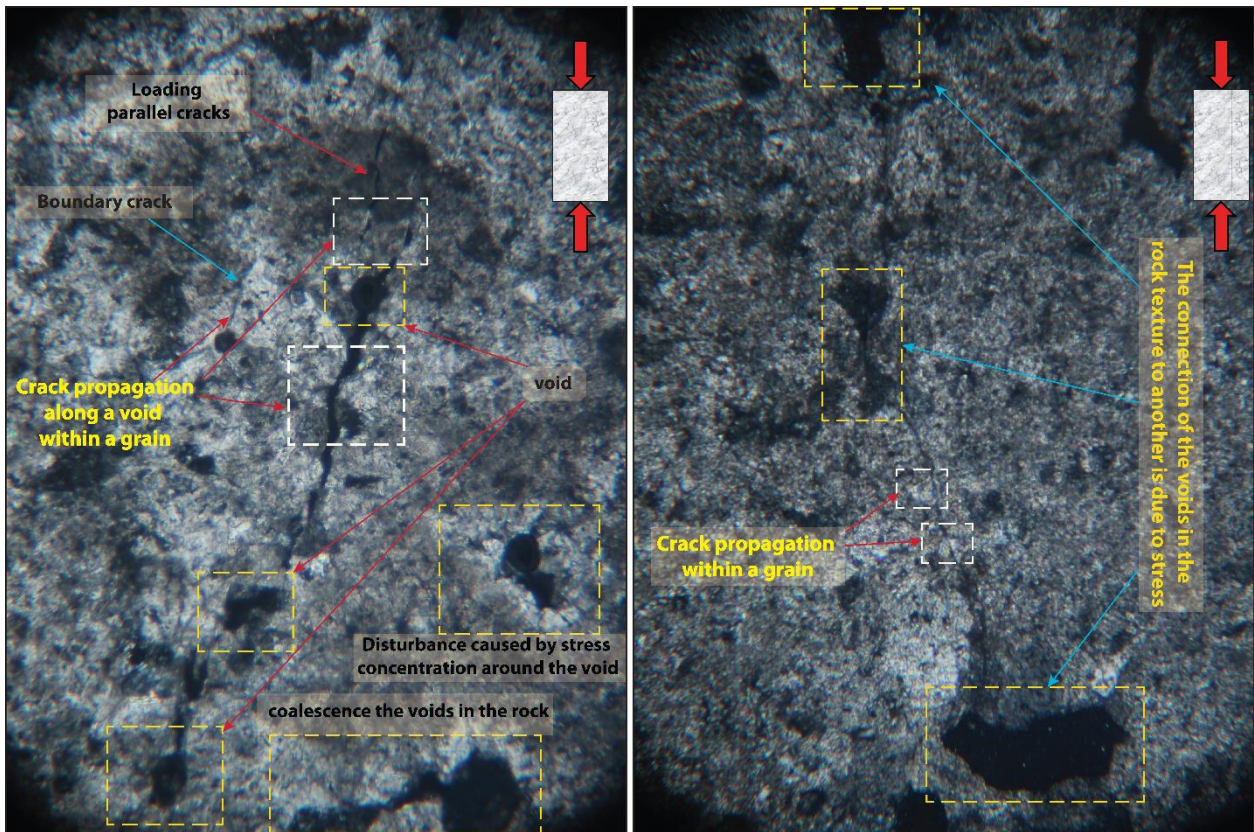


Fig. 5: The photomicrograph of the crack caused by stress in limestone

directions on the loading axis, and also the measurement of shear wave velocity ( $V_s$ ), can also be of considerable help in this regard.

The initiation and propagation of micro-cracks under stress, strongly depends on the mineralogy, the fabric and the microstructure of the rocks. Some researchers have attempted to find the effect of microstructures on mechanical and physical parameters of the rock. Kranz (1983) divided the micro-cracks of rocks into four types: (1) boundary cracks, (2) intra-granular cracks formed within a grain, (3) inter-granular cracks extending from the grain boundaries to a grain, (4) trans-granular cracks extending through the grain boundaries and crossing several grains [31]. The mechanical behavior of the rocks varies by changing the type and amount of micro-cracks subjected to loading. For this purpose, in the present study, a microscopic thin-section was prepared from the limestone parallel with the loading direction after the ultimate failure. As shown in Fig. 5, by placing the rock under stress, the cracks initiate and propagate approximately parallel with the applied load (0-10). According to the observations in the studied limestone, the pores are less frequent, but relatively large in size. It is also observed that due to loading around the pores, stress concentration has occurred and cracks have propagated around the pores and penetrated into the grains. In other words, it was observed that in most cases subjected to stress, cracks initiate around the pores in the rock. By increasing the load and overcoming the resistance of the bond between the grains and the penetration into the grains, the interconnected network of cracks is created inside the rock.

Therefore, coalescence and bonding of pores finally lead to macroscopic fracture in the rock. According to what has been said, in the studied limestone there is a set of boundary, intra-granular, inter-granular and trans-granular cracks.

#### 4. CONCLUSION

This paper evaluated the effect of the crack initiation and propagation process on the pressure wave velocity due to compressive loading. Based on the results, the pressure wave velocity variations for both types of rock (limestone and plaster stone) can be divided into two important stages: (1) in the first stage, the pressure wave velocity is increased with increasing loading to a certain stress level and then (2) with a higher loading, the pressure wave velocity will decrease suddenly and severely. The pressure wave velocity for limestone initially reaches a stress level of 50% of the peak strength by about 5%, and then decreases by about 50%. Similarly, in plaster artificial stone, the wave velocity increased by about 1.6% up to the loading level of 70% and then suddenly decreased. Also, by studying the microscopic thin sections prepared after the ultimate failure of limestone, it was observed that the stress concentration occurred around the pores due to the loading and the crack around the pores has propagated and penetrated into the grain. According to the observations, these cracks initiate and propagate approximately parallel with the load applied.

#### REFERENCE

- [1] Martin C, Chandler N. The progressive fracture of Lac du Bonnet granite.

- International Journal of Rock Mechanics and Mining Sciences & Geomechanics Abstracts: Elsevier; 1994. p. 643-59.
- [2] Brace W, Paulding B, Scholz C. Dilatancy in the fracture of crystalline rocks. *Journal of Geophysical Research*. 1966;71:3939-53.
- [3] Bieniawski ZT. Mechanism of brittle fracture of rock: part II—experimental studies. *Int J Rock Mech Min & Geomech Abstr*. 1967;4:395-404.
- [4] Horii H, Nemat-Nasser S. Compression-induced microcrack growth in brittle solids: Axial splitting and shear failure. *Journal of Geophysical Research: Solid Earth*. 1985;90:3105-25.
- [5] Hoek E, Bieniawski Z. Brittle fracture propagation in rock under compression. *International Journal of Fracture Mechanics*. 1965;1:137-55.
- [6] Dyskin A, Sahouryeh E, Jewell R, Joer H, Ustinov K. Influence of shape and locations of initial 3-D cracks on their growth in uniaxial compression. *Engineering Fracture Mechanics*. 2003;70:2115-36.
- [7] Dyskin A, Germanovich L, Jewell R, Joer H, Krasinski J, Lee K, et al. Some experimental results on three-dimensional crack propagation in compression. *Proceedings of the 1995 2nd International Conference on the Mechanics of Jointed and Faulted Rock-MJFR-2 New York:[sn]1995. p. 91-6.*
- [8] Eberhardt E, Stead D, Stimpson B. Quantifying progressive pre-peak brittle fracture damage in rock during uniaxial compression. *International Journal of Rock Mechanics and Mining Sciences*. 1999;36:361-80.
- [9] Meng Q, Zhang M, Han L, Pu H, Li H. Effects of size and strain rate on the mechanical behaviors of rock specimens under uniaxial compression. *Arabian Journal of Geosciences*. 2016;9:527.
- [10] Keller A. High resolution, non-destructive measurement and characterization of fracture apertures. *International Journal of Rock Mechanics and Mining Sciences*. 1998;35:1037-50.
- [11] Zang A, Christian Wagner F, Stanchits S, Dresen G, Andresen R, Haidekker MA. Source analysis of acoustic emissions in Aue granite cores under symmetric and asymmetric compressive loads. *Geophysical Journal International*. 1998;135:1113-30.
- [12] Klobes P, Riesemeier H, Meyer K, Goebbels J, Hellmuth K-H. Rock porosity determination by combination of X-ray computerized tomography with mercury porosimetry. *Fresenius' journal of analytical chemistry*. 1997;357:543-7.
- [13] Martínez-Martínez J, Fusi N, Galiana-Merino JJ, Benavente D, Crosta GB. Ultrasonic and X-ray computed tomography characterization of progressive fracture damage in low-porous carbonate rocks. *Engineering Geology*. 2016;200:47-57.
- [14] Crosta G, Agliardi F, Fusi N, Zanchetta S, Barberini V, Laini M, et al. Rock fabric controls on the failure mode of strongly deformed gneisses. *Rock Mechanics in Civil and Environmental Engineering: Taylor & Francis Leiden*; 2010. p. 107-10.
- [15] Ketcham RA. Three-dimensional grain fabric measurements using high-resolution X-ray computed tomography. *Journal of Structural Geology*. 2005;27:1217-28.
- [16] Hirono T, Takahashi M, Nakashima S. In situ visualization of fluid flow image within deformed rock by X-ray CT. *Engineering Geology*. 2003;70:37-46.
- [17] Vervoort A, Wevers M, Swennen R, Roels S, Van Geet M, Sellers E. Recent advances of X-ray CT and its applications for rock material. *X-ray CT for Geomaterials Soils, Concrete, Rocks Balkema Publ*. 2004:79-91.
- [18] Ohtani T, Nakano T, Nakashima Y, Muraoka H. Three-dimensional shape analysis of miarolitic cavities and enclaves in the Kakkonda granite by X-ray computed tomography. *Journal of Structural Geology*. 2001;23:1741-51.
- [19] Tziallas G, Tsiambaos G, Saroglou H. Determination of rock strength and deformability of intact rocks. *Electronic Journal of Geotechnical Engineering*. 2009;14:e12.
- [20] Zhao J, Cai J, Zhao X, Li H. Experimental study of ultrasonic wave attenuation across parallel fractures. *Geomechanics and Geoengineering: An International Journal*. 2006;1:87-103.
- [21] Nasser M, Schubnel A, Young R. Coupled evolutions of fracture toughness and elastic wave velocities at high crack density in thermally treated Westerly granite. *International Journal of Rock Mechanics and Mining Sciences*. 2007;44:601-16.
- [22] El Azhari H, El Hassani I-EEA. Effect of the number and orientation of fractures on the P-wave velocity diminution: application on the building stones of the Rabat Area (Morocco). *Geomaterials*. 2013;3:71.
- [23] ISRM. Suggested method for determining Water Content, Porosity, Density, Absorption and Related Properties and Swelling and Slake-durability Index Properties. 1979. p. 141-56.
- [24] ISRM. Suggested methods for determining the uniaxial compressive strength and deformability of rock materials. *Rock characterization, testing and monitoring—ISRM suggested methods*. 1981. p. 113-6.
- [25] ISRM. Upgraded ISRM suggested method for determining sound velocity by ultrasonic pulse transmission technique. 2014. p. 255-9.
- [26] Akesson U, Hansson J, Stigh J. Characterisation of microcracks in the Bohus granite, western Sweden, caused by uniaxial cyclic loading. *Engineering Geology*. 2004;72:131-42.
- [27] Hadley K. Comparison of calculated and observed crack densities and seismic velocities in Westerly granite. *Journal of Geophysical Research*. 1976;81:3484-94.
- [28] Rigopoulos I, Tsikouras B, Pomonis P, Hatzipanagiotou K. Microcracks in ultrabasic rocks under uniaxial compressive stress. *Engineering Geology*. 2011;117:104-13.
- [29] Rigopoulos I, Tsikouras B, Pomonis P, Hatzipanagiotou K. Petrographic investigation of microcrack initiation in mafic ophiolitic rocks under uniaxial compression. *Rock mechanics and rock engineering*. 2013;46:1061-72.
- [30] Heap M, Faulkner D, Meredith P, Vinciguerra S. Elastic moduli evolution and accompanying stress changes with increasing crack damage: implications for stress changes around fault zones and volcanoes during deformation. *Geophysical Journal International*. 2010;183:225-36.
- [31] Kranz RL. Microcracks in rocks: a review. *Tectonophysics*. 1983;100:449-80.

#### HOW TO CITE THIS ARTICLE

T. Asheghi Mehmadari, A. Fahimifar, F. Asemi, *The Effect of the Crack Initiation and Propagation on the P-Velocity of Limestone and Plaster Subjected to Compressive Loading*, *AUT J. Civil Eng.*, 4(1) (2020) 55-62.

DOI: [10.22060/ajce.2019.15984.5558](https://doi.org/10.22060/ajce.2019.15984.5558)



